Condensed Matter Physics, 2015, Vol. 18, No 3, 33801: 1–7
DOI: 10.5488/CMP.18.33801
http://www.icmp.lviv.ua/journal

CONDENSED MATTER PHYSICS

Elastic properties of 5d transition-metal carbides: An *ab initio* study

L. Mex[1], A. Aguayo[2], G. Murrieta[2]

[1] Facultad de Ingeniería, Universidad Autynoma de Yucatán. Av. Industrias no Contaminantes por Periférico Norte Apdo. Postal 150 Cordemex Mérida, Yucatán, México

[2] Facultad de Matemáticas, Universidad Autynoma de Yucatán. Periférico Norte, Tablaje 13615, C. P. 97110, Mérida, Yucatán, México

Received December 9, 2014, in final form April 14, 2015

We have systematically studied the mechanical stability of group V transition metal carbides TMC_2 (TM = Hf, Ta, W, Re, Os, Ir, Pt, and Au) in the pyrite and fluorite phase, by calculating their elastic constants within the density functional theory scheme. It was found that all but ReC_2 and OsC_2 are stable in pyrite phase. On the other hand, all metal carbides studied were unstable in the fluorite phase.

Key words: *first-principles calculation, elastic constants, hard material, transition metals*

PACS: *81.05.Je, 81.05.Zx, 71.15.Mb, 71.20.Be*

1. Introduction

The elastic stability criterion has been used to establish the possible stability or metastability of a crystallographic phase in the solid state. It has been shown that through the first-principles calculation it is possible to obtain the elastic properties and to describe the strength of the bond between neighboring atoms. Since the adequacy of the theoretical results made it possible to adequately predict the formation of new crystal structures, it became possible to synthesize some of the predicted structures.

Intensive theoretical and experimental efforts have been focused on the possibility of finding new low compressibility materials with hardness comparable with diamond [1]. Superhard materials are of primary importance in modern science and technology due to their numerous applications, starting from cutting and polishing tools up to wear resistant coatings. In this search, special interest has been taken in the metal carbides and nitrides. The introduction of smaller atoms such as nitrogen or carbon into interstitial sites in closely packed transition metal lattices changes their chemical and physical properties with respect to the metal. Transition metal carbides and nitrides have been considerably investigated due to their unique chemical and physical properties, such as high thermal conductivity, high melting point, chemical inertness, high stiffness, high hardness, and metallic electrical conductivity [2–7]. Transition metal carbides or nitrides had been little studied due to the difficulty of obtaining the crystalline samples. However, a series of works such as PtN, PtN_2, IrN_2, and PtC [8] triggered a rapid advance in the production of new carbide and nitride materials. They can have different morphologies, atomic structures and substantially differ from the corresponding crystalline phase relative to their physicochemical properties. To date, a wide group of nanocarbides of the d metals such as molecular clusters, nanocrystals, nanospheres, nanowires, nanotubes, etc., have been synthesized. Several of these new systems formed by transition metals and nitrogen or carbon have found no consensus on their crystal structure. Among all these materials, the group of platinoid nitrides and carbides attracted a particular interest due to their technological potential. Crowhurst et al. [9] in order to explain the high bulk modulus of platinum nitrides studied the Pt–N system in the stoichiometry PtN_2. They analyzed the composite in two different structures, fluorite and pyrite, and found that the most stable phase is the pyrite phase, with an internal parameter $u = 0.415$.

To explore the possible existence of $5d$ transition-metal carbides with C/M = 2 stoichiometry in the pyrite or fluorite phases, using density functional theory, we calculated the elastic constants in both cubic phases and analyzed the performance of elastic stability criteria.

2. Methods

The first-principles calculations were performed based on the density functional theory (DFT). The Kohn-Sham total energies were self-consistently calculated using the linearized augmented plane wave method (FP-LAPW) with local orbital extensions [10], as implemented in the WIEN2k [11, 12] code, where the core states are treated fully relativistically, and the semicore and valence states are computed in a scalar relativistic approximation. The exchange-correlation terms were considered in the Perdew-Burke-Ernzerhof form of the generalized gradient approximation (GGA) [13]. We have chosen the muffin-tin radii (R_{MT}) of 2.0 a.u. for the transition metals and 1.2 a.u. for the carbon atoms. The self-consistent calculations were done with an LAPW basis set defined by the cutoff $R_{MT}K_{MAX}$=8.0. Inside the atomic spheres, the potential and charge densities are expanded in crystal harmonics up to $L = 10$. Convergence was assumed when the energy difference between the input and output charge densities was less than 1×10^{-5} Ry. The calculations were carried out with a sufficiently large number of **k** points in the first Brillouin zone (BZ). We used a $13 \times 13 \times 13$ **k**-point mesh, yielding a different number of **k** points in the irreducible wedge of the BZ depending on the structure: 256 for the fluorite, and 176 for the pyrite phase.

We evaluated the structure of TMC_2 (TM=Hf, Ta, W, Re, Os, Ir, Pt, and Au) in the pyrite and fluorite phase. Pyrite (FeS_2 structure type) has a cubic crystal structure with space group $Pa\overline{3}$ (205), the transition metal atoms occupying Wyckoff site $4a$ (0,0,0), and the carbon atoms are grouped as dimers around the fcc octahedral interstitial sites oriented in the $\langle 111 \rangle$ directions at $8c$ (u, u, u). The transition metal in the pyrite structure is fixed by symmetry but the carbon atoms have one free parameter (u) [14]. Fluorite is a particular high symmetry phase of pyrite. When the free parameter $u = 0.25$ at the 8c site, we obtain the fluorite (CaF_2 structure type) structure with space group cF12 (225).

The calculated total energy as a function of volume was fitted to the Birch–Murnaghan equation of state [15]. From this process, the equilibrium lattice constant (a) and the bulk modulos (B) were obtained. All crystals in a cubic structure have only three independent elastic constants, namely C_{11}, C_{12}, and C_{44}. One can use a small strain and calculate the change of energy or stress to obtain elastic constants C_{ij}. In the crystal structures analyzed in this work, an external strain δ from -0.08 to + 0.08 was applied in the directions as explained by Güemez et al. [16], associated with deformations: isotropic, tetragonal and orthorhombic.

$$\epsilon_{\text{iso}} = \begin{pmatrix} (1+\delta)^{1/3} & 0 & 0 \\ 0 & (1+\delta)^{1/3} & 0 \\ 0 & 0 & (1+\delta)^{1/3} \end{pmatrix},$$

$$\epsilon_{\text{tet}} = \begin{pmatrix} (1+\delta)^{-\frac{1}{3}} & 0 & 0 \\ 0 & (1+\delta)^{-\frac{1}{3}} & 0 \\ 0 & 0 & (1+\delta)^{\frac{2}{3}} \end{pmatrix}, \tag{1}$$

$$\epsilon_{\text{ort}} = \begin{pmatrix} 1 & \delta & 0 \\ \delta & 1 & 0 \\ 0 & 0 & 1+\delta^2 \end{pmatrix},$$

to distort the lattice vectors, $R' = (1 + \epsilon)R$. The resulting changes of energy are associated with elastic constants,

$$\Delta E_{\text{iso}} = \frac{V_0}{2}(C_{11} + 2C_{12})\delta^2 = \frac{2V_0}{3}B\delta^2,$$

$$\Delta E_{\text{tet}} = \frac{V_0}{3}(C_{11} - C_{12})\delta^2 \quad \text{and}$$

$$\Delta E_{\text{ort}} = 2V_0 C_{44}\delta^2.$$

In order to be mechanically stable, the elastic stiffness constants of a given crystal should satisfy the generalized elastic stability criteria [17]. The elastic stability criteria for a cubic crystal at ambient conditions are,

$$C_{11} + 2C_{12} > 0, \quad C_{11} - C_{12} > 0, \quad \text{and} \quad C_{44} > 0, \tag{2}$$

i.e., all the bulk moduli (B), shear (C_{44}), and tetragonal shear [$C' = (C_{11} - C_{12})/2$] moduli are positive. We also calculated the Young's modulus (E), which provides a measure of stiffness and stability of the solids. Another interesting elastic property for any applications, particularly for their anisotropy, is the Zener factor A. These quantities are calculated in terms of the computed C_{ij} using the following relations

$$E = \frac{9BG}{3B + G}, \tag{3}$$

$$A = \frac{C_{44}}{C'} = \frac{2C_{44}}{C_{11} - C_{12}}, \tag{4}$$

where G is the isotropic shear modulus. For a cubic material with its two shear constants, C_{44} and C', the value of G should be between these two constants. Therefore, G has a unique value if $C_{44} = C'$. This happens if the material is isotropic, that is, the Zener factor is equal to one, as in the case of W. By assuming a homogeneous strain on the compound, Voigth [18] established the upper limit of G as

$$G\text{V} = \frac{1}{5}C'(2 + 3A). \tag{5}$$

On the other hand, assuming a homogeneous stress, as the lower bound Reuss [19] proposes

$$G\text{R} = 5C'\frac{A}{3 + 2A}. \tag{6}$$

In this work, we take the arithmetic average as proposed by Hill [20]

$$G = \frac{1}{2}(G\text{V} + G\text{R}). \tag{7}$$

3. Results and discussion

In figure 1 we show the calculated total energy of pyrite HfC_2 and AuC_2 (pyrite-face) for seven values of the cell volume (open circles). The calculated total energy as a function of volume was fitted to the Birch-Murnaghan equation of state[15]. The fit is presented in figure 1 (solid line), were the energy is given with respect to the minimum energy of the pyrite structure.

In order to find the value of the free parameter u in the pyrite phase, the DFT total energy and the forces acting on the atoms were optimized. Figure 2 shows the DFT total energy as a function of the free parameter u for HfC_2. In this curve, we have got two local minima, one of them being observed at $u = 0.25$, which correspond to a possible metastable fluorite phase. At $u = 0.43$, there is another minimum at much lower energy, which corresponds to pyrite phase. In all the 5d transition metal carbides studied in this work, we have got the same value for the free parameter u. The difference in the energy between the two minimum phase suggests that pyrite phase should be a more stable phase at zero pressure.

From the analysis of elastic stability, applying a standard set of deformations [equation (1)], we find that all compounds in fluorite phase are unstable, particularly under the tetragonal deformation, that is, the relation $C_{11} - C_{12}$ turned out to be negative.

The table 1 presents the results of our calculations for the pyrite phase. Our results demonstrate that HfC_2, TaC_2, WC_2, IrC_2, PtC_2 and AuC_2 are mechanically stable, while ReC_2 and OsC_2 violate the mechanical stability conditions. In both of them, the shear modulus (C_{44}) was negative, so the shear modulus C_{44} is the main constraint on stability in those compounds in the pyrite phase. As can be seen, in general it holds for pyrite phase that $B > C' > C_{44} > 0$.

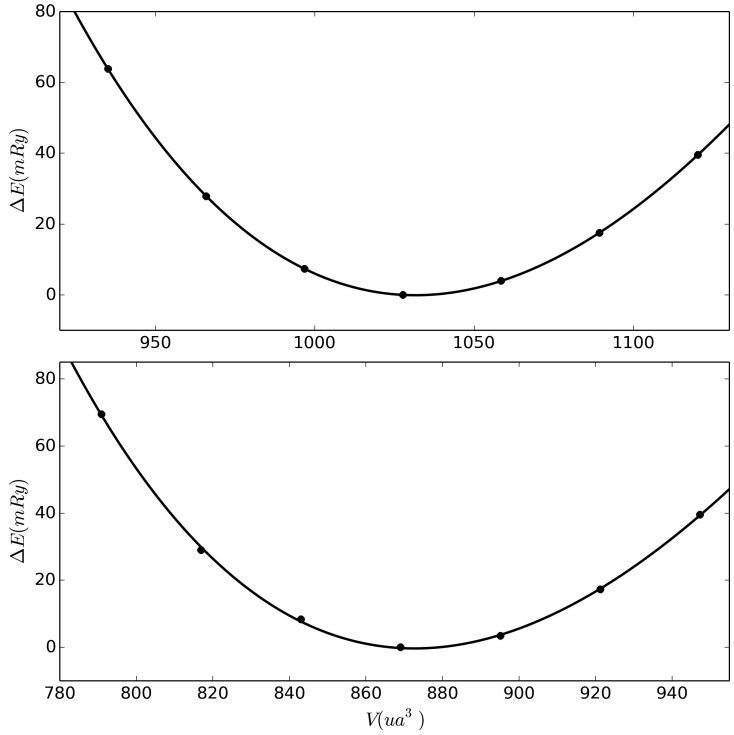

Figure 1. Calculated total energies for HfC_2(top) and AuC_2(bottom) under isotropic deformation (circles). The energy of the pyrite phase at the equilibrium volume is the reference level, and is set to zero. The line corresponds to a fit of the Birch-Murnaghan equation of state to the calculated energy values (see text).

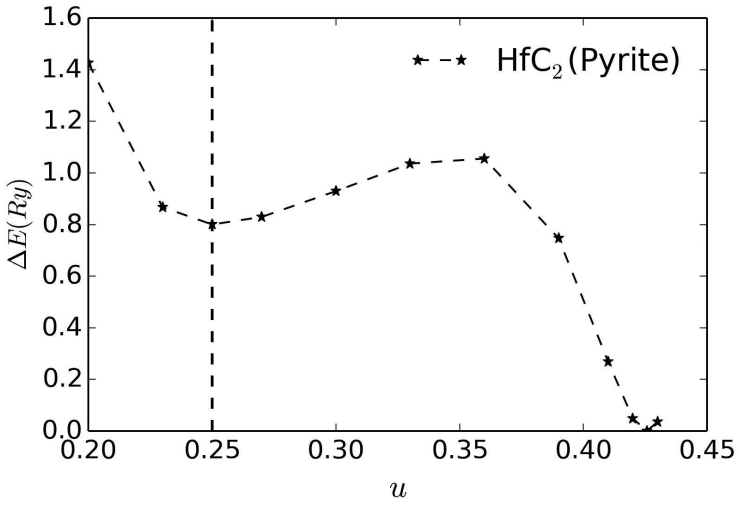

Figure 2. Energy of HfC_2 as a function of the position of C atoms (u). When $u = 1/4$, HfC_2(pyrite) reduces to HfC_2(fluorite). For all the transition metal carbides studied in this work, the second minimum was in $u = 0.43$

The Zener anisotropy factor A is a measure of the degree of elastic anisotropy in solids. A will take the value of 1 for a completely isotropic material. A value of A smaller or greater than unity shows the degree of elastic anisotropy. The calculated Zener anisotropy for pyrite structure (see table 1) implies that all compounds are elastically anisotropic (A <1). In order to better visualize the anisotropy of these

Table 1. DFT lattice constant a, zero pressure elastic constants c_{ij} (GPa), bulk modulus B_0 (GPa), shear modulus G (GPa), Zener factor A, and Young's modulus (GPa), calculated in the present work for pyrite phase of period VI transition metal carbides.

	a(Å)	C_{11}	C_{12}	C_{44}	B_0	G	A	E
HfC_2	5.34	275	127	53	176	61	0.72	158
TaC_2	5.12	380	168	71	238	83	0.67	217
WC_2	5.03	432	183	30	266	55	0.24	152
ReC_2	4.98	Unstable	Unstable	Unstable	282	–	–	–
OsC_2	4.96	Unstable	Unstable	Unstable	286	–	–	–
IrC_2	4.95	569	133	69	279	112	0.32	289
PtC_2	4.98	603	101	88	268	136	0.35	342
AuC_2	5.06	445	102	116	217	135	0.68	326

compounds, we show a three-dimensional (3D) representation of Young's modulus. For cubic crystals, the directional dependence of the Young's modulus in 3D representation can be given by

$$\frac{1}{E} = S_{11} - 2\left(S_{11} - S_{12} - \frac{1}{4}S_{44}\right)\left(l_1^2 l_2^2 + l_2^2 l_3^2 + l_3^2 l_1^2\right), \tag{8}$$

where S_{ij} are the elastic compliance constants, and l_1, l_2 and l_3 are the directional cosines to the $x-$, $y-$ and $z-$axes, respectively. In the ⟨100⟩ directions, the second term is zero, and for $C_{44}/C' < 1$, a maximum in ⟨100⟩ directions. In all the compounds, the Zener's coefficient was less than one, so that ⟨111⟩ directions are soft and ⟨100⟩ are hard. Three-dimensional representation of Young's modulus is shown in figure 3. It can be seen that the elastic anisotropy increases in the direction ⟨100⟩ as Zener's coefficient decreases.

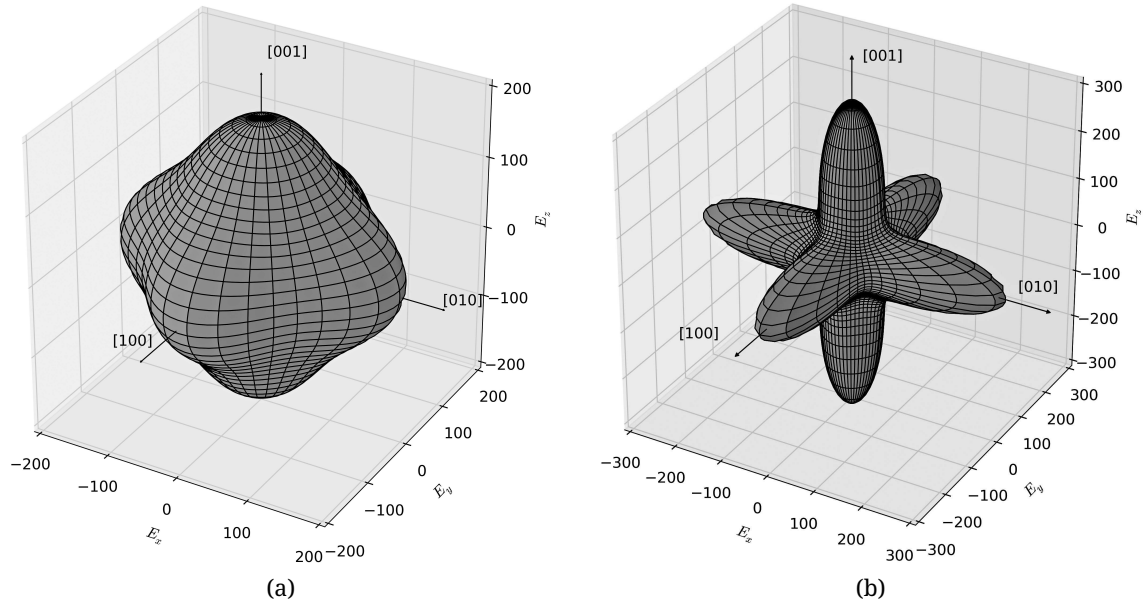

Figure 3. 3D directional dependence of the Young's modulus for (a) AuC_2 (A = 0.68) and (b) WC_2 (A = 0.24).

The bulk moduli follow the parabolic behavior, and increases from HfC_2 to reach the maximum on IrC_2. This behavior is similar to that present in the corresponding 5d transition metals. However, not all compounds, the bulk modulus increases relative to that of the pure elements, as in the case of nitrides. The values of the bulk modulus increase in: HfC_2 (from 109 GPa to 176 Gpa), TaC_2 (from 200 GPa to 238 GPa), PtC_2 (from 230 to 268), and AuC_2 (from 173 to 217). On the other hand, the other two stable

compounds in the pyrite phase show a decrease in the bulk modulus compared to that of pure transition metals: WC_2 from 323 GPa to 266 GPa, and IrC_2 from 355 GPa to 279 GPa. This same trend is followed by the Young's modulus with an increasing value in the dicarbides with Hf, Ta, Pt and Au.

The generally accepted rule is to associate hard compounds with high bulk and shear modulus values [21]. However, bulk modulus is not the only mechanical quantity that determines the utility of a material for hard coatings. Another important material property to be also considered is toughness, which is influenced by the degree of plastic deformation (ductility) of the material under mechanical loading. To analyze the ductility of the compounds, we use the Pettifor's criterion [22, 23], which states that, for metallic non-directional bonding compounds, the Cauchy pressure ($C_{12} - C_{44}$) value is typically positive. This region corresponds to a ductile behavior of a material. The other criterion we used was the Pugh's modulus ratio G/B, If G/B > 0.57[24], and the materials behave in a brittle manner. In figure 4, we show the Pugh and Pettifor criteria to map the ductility and brittle behavior for pyrite phase of period VI transition metal carbides. According to their formulation, the only compound which is not within the ductile region of the map is AuC_2.

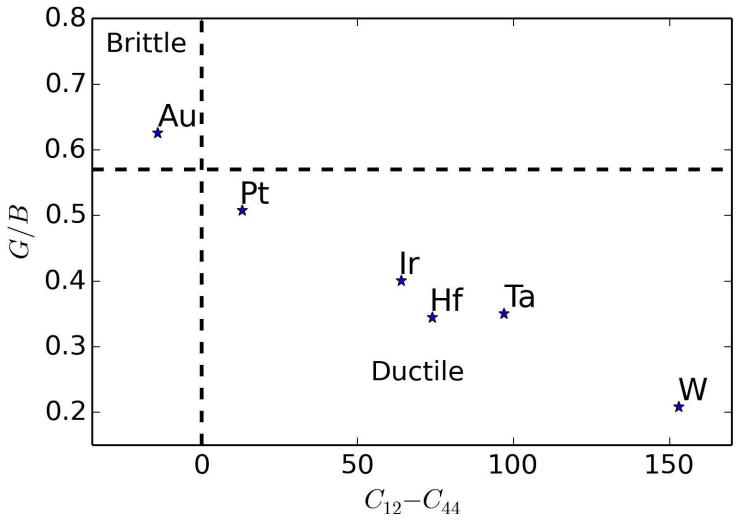

Figure 4. Map of brittleness and ductility trends of HfC_2, TaC_2, WC_2, IrC_2, PtC_2, and AuC_2. In the figure, only the transition metal simbol is shown.

4. Conclusion

In summary, we have studied metal carbides TMC_2 in the fluorite and pyrite structures using first-principles calculations. With all the calculations, we conclude that all metal carbides studied with fluorite structure are mechanically unstable. On the other hand, the pyrite phase for ReC_2 and OsC_2 does not meet the stability criteria as well. The bulk and Young's moduli value increases to the value of the pure elements in HfC_2, TaC_2, PtC_2, and Au_2, but decreases in WC_2 and IrC_2. According to the criterion of brittleness (ductility), all compounds except AuC_2 exhibit a ductility behavior.

Acknowledgements

The authors would like to thank Carlos Brito for helpful comments. This work was supported by Facultad de Matámaticas-UADY under Grant no. FMAT–2012–0007 and CONACyT under Grant no. 025794.

References

1. Seung H.J., Jisoon I., Steven G.L., Marvin L.C., Nature, 1999, **399**, 367; doi:10.1038/20148.
2. Sahnoun M., Daul C., Driz M., Parlebas J.C., Demangeat C., Computational Materials Science, 2005, **33**, 175; doi:10.1016/j.commatsci.2004.12.010.
3. Friedrich A., Winkler B., Juarez-Arellano E.A., Lkhamsuren B., Materials, 2011, **4**, 1648; doi:10.3390/ma4101648.
4. Friedrich A., Winkler B., Bayarjargal L. Morgenroth W., Juarez-Arellano E.A. Milman V., Refson K., Kunz M., Chen K., Phys. Rev. Lett., 2010, **8**, 085504; doi:10.1103/PhysRevLett.105.085504.
5. Srivastava A., Diwan B.D., Can. J. Phys., 2012, **90**, 331; doi:10.1139/p2012-021.
6. Chauhan M., Gupta D.C., Diam. Relat. Mater., 2013 **40**, 96; doi:10.1016/j.diamond.2013.10.011.
7. Srivastava A. Chauhan M. Singh R.K., Phase Transition, 2011 **84**, 58; doi:10.1080/01411594.2010.509644.
8. Ono S., Kikegawa T., Ohishi Y., Solid State Commun., 2005, **133**, 55; doi:10.1016/j.ssc.2004.09.048.
9. Crowhurst J.C., Goncharov A.F., Sadigh B., Evans C.L., Morrall P.G., Ferreira J.L., Nelson A.J., Science, 2006, **311**, 1275; doi:10.1126/science.1121813 .
10. Singh D.J., Nordstrom L., Planewaves, Pseudopotentials and the LAPW Method, Springer, 2006; doi:10.1007/978-0-387-29684-5.
11. Blaha P., Schwarz K., Madsen G., Kvasnicka D., Luitz J., WIEN2k An Augmented PlaneWave + Local Orbitals Program for Calculating Crystal Properties, Vienna University of Technology Inst. of Physical and Theoretical Chemistry, Austria, 2013.
12. Schwarz K., Blaha P., Comp. Mater. Sci., 2003, **28**, 259; doi:10.1016/S0927-0256(03)00112-5.
13. Perdew J.P., Burke K., Ernzerhof M., Phys. Rev. Lett., 1996, **77**, 3865; doi:10.1103/PhysRevLett.77.3865.
14. Birkholz M., J. Phys. Condens. Mat., 1992, **4**, 6227; doi:10.1088/0953-8984/4/29/007.
15. Birch F., Phys. Rev., 1947, **71**, 809; doi:10.1103/PhysRev.71.809.
16. Güemez A., Murrieta G., Aguayo A., Abstraction & Application, 2011, **4**, 1.
17. Wang J., Yip S., Phillpot S.R. Wolf D., Phys. Rev. Lett., 1993, **71**, 4182; doi:10.1103/PhysRevLett.71.4182.
18. Voight W., Lehrbuch der kristallphysik (mit ausschluss der kristalloptik), Springer-Verlag, Leipzig, 1928.
19. Reuss A., Angew Z., Math. Mech., 1929, **9**, 49.
20. Hill R., P. Phys. Soc. A, 1952, **65**, 349; doi:10.1088/0370-1298/65/5/307.
21. Haines J., Bocquillon G., Ann. Rev. Mater. Res., 2001, **31**, 1; doi:10.1146/annurev.matsci.31.1.1.
22. Pettifor D.G., Mater. Sci. Tech., 1992, **8**, 345; doi:10.1179/mst.1992.8.4.345.
23. Sangiovanni D.G., Hultman L., Chirita V., Acta Mater., 2011, **59**, 2121; doi:10.1016/j.actamat.2010.12.013.
24. Pugh S.F., Philos. Mag. Ser. 7, 1954, **45**, 823; doi:10.1080/14786440808520496.

Еластичні властивості карбідів 5d перехідних металів: *ab initio* дослідження

Л. Мекс[1], А. Агуайо[2], Г. Муррієта[2]

[1] Інженерний факультет, Автономний університет Юкатану, Юкатан, Мексика

[2] Факультет математики, Автономний університет Юкатану, Юкатан, Мексика

Проведено систематичні дослідження менханічної стійкості карбідів перехідних металів п'ятої групи TMC_2 (TM = Hf, Ta, W, Re, Os, Ir, Pt, і Au) у піритовій і флюоритовій фазах шляхом обчислення їх еластичних сталих в рамках теорії функціоналу густини. Встановлено, що всі карбіди металів, за винятком ReC_2 і OsC_2, є стійкими у піритовій фазі. З іншого боку, всі метали карбідів, що вивчалися, виявилися нестійкими у флюоритовій фазі.

Ключові слова: *першопринципні обчислення, еластичні стали, твердий матеріал, перехідні метали*